

**SURVEY AND LOGISTICS REPORT
ON A HELICOPTER BORNE
VERSATILE TIME DOMAIN
ELECTROMAGNETIC (VTEM)
SURVEY**

on the

**TASMANIA PROJECT AREA
AUSTRALIA**

for

ZINIFEX LIMITED

by



GEOTECH AIRBORNE LIMITED

Unit 1 / 29 Mulgul Road
MALAGA WA 6090
Tel: +61 (0) 8 9249 8814
Fax: +61 (0) 8 9249 8894
www.geotechairborne.com.au
e-mail: info@geotechairborne.com

**Project A371
August, 2008**

TABLE OF CONTENTS

1. SURVEY SPECIFICATIONS.....	3
1.1. General.....	3
1.2. VTEM flight plan on Google EARTH™ Background	3
1.3. Survey block coordinates.	4
1.4. Survey block specifications	5
1.5. Survey schedule	5
2. SYSTEM SPECIFICATIONS.....	6
2.1. Instrumentation.....	6
2.2. VTEM Configuration	7
2.3. VTEM decay sampling scheme	7
2.4. VTEM Transmitter Waveform over one half-period.....	8
3. PROCESSING.....	9
3.1. Processing parameters.....	9
3.2. Flight Path.....	9
3.3. Electromagnetic Data	9
3.4. Magnetic Data	9
3.5. Digital Terrain Model	10
4. DELIVERABLES.....	11
5. PERSONNEL.....	13

APPENDICES

A. Modeling VTEM data	14
B. Geophysical Maps	20



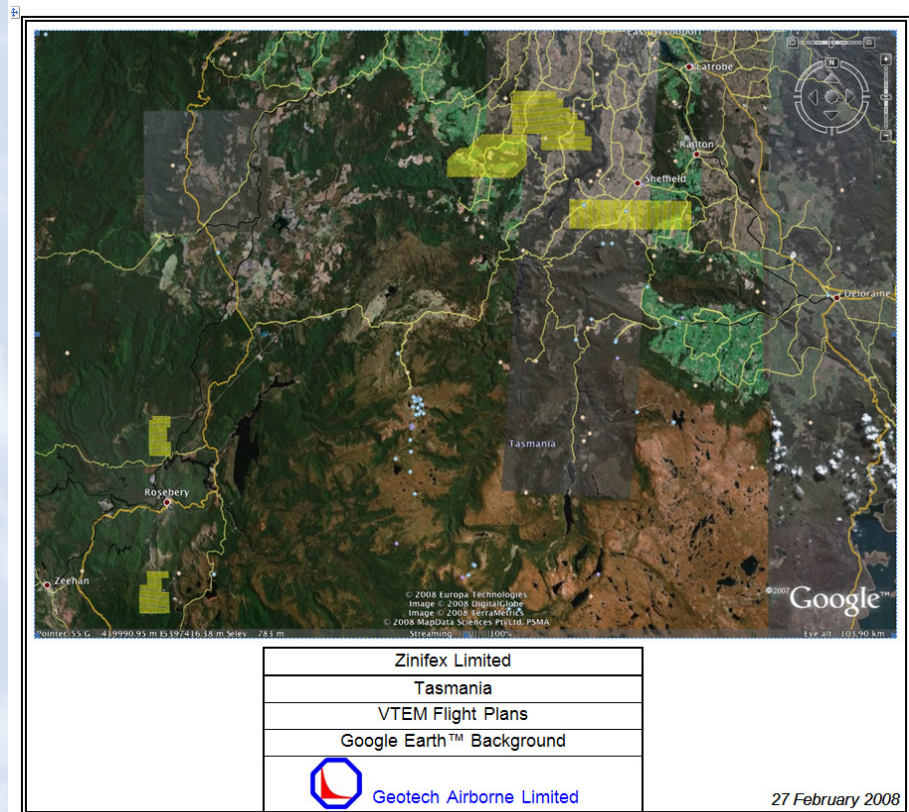
SURVEY AND LOGISTICS REPORT ON A HELICOPTER-BORNE VTEM SURVEY

1. SURVEY SPECIFICATIONS

1.1. General

Job Number	A371
Client	Zinifex Limited
Project Area	Tasmania
Location	Tasmania
Number of Blocks	5
Total line kilometres	1129
Survey date	17 March to 7 April, 2008
Client Representative	Julius Marinelli Tel: +61 3 9288 0333, Fax: +61 3 9288 0406 Julius.Marinelli@Zinifex.com
Client address	Level 29, Freshwater Place, 2 Southbank Boulevard, Southbank VIC, 3006, Australia
Client Consultant (if applicable)	Dr Jovan Silic, Flagstaff GeoConsultants (JSA Pty Ltd) Tel: +61 (0) 3 9867 8931, Fax: (0) 3 8420 6299 jsilic@bigpond.com

1.2. VTEM flight plan on Google EARTH™ Background



1.3. Survey blocks coordinates.

Easting UTM Z 55S	Northing UTM Z 55S
BLOCK 1	
376108.9	5364205
379101.6	5364179
379111.3	5363186
378109.2	5363188
378114.5	5361191
379109.3	5361179
379102.9	5358170
375104.2	5358187
375105.9	5362191
376115.3	5362179
376108.9	5364205

Easting UTM Z 55S	Northing UTM Z 55S
BLOCK 2	
376603.4	5385695
379105.7	5385689
379109.4	5384185
378610.7	5384176
378601.2	5382180
379107.2	5382178
379111.8	5380192
376105.7	5380188
376113	5385195
376612	5385194
376603.4	5385695

Easting UTM Z 55S	Northing UTM Z 55S
BLOCK 3	
420139.7	5425181
428107.8	5425190
428092.9	5419160
417084.2	5419216
417113.3	5423211
420104.6	5423270
420139.7	5425181

Easting UTM Z 55S	Northing UTM Z 55S
BLOCK 4	
426093.2	5431206
432095.7	5431205
432116	5430218
433127.6	5430198
433136.9	5429182



434103.5	5429205
434123.7	5428204
435134.9	5428198
435121.6	5427196
436110.2	5427205
436150.2	5425187
437127.5	5425196
437122.8	5423177
430105.5	5423187
430063.8	5425205
426099.2	5425165
426093.2	5431206

Easting UTM Z 55S	Northing UTM Z 55S
BLOCK 5	
434099.9	5416240
451099.2	5416201
451126.2	5412207
434099.2	5412221
434099.9	5416240

1.4. Survey blocks specifications

Survey block	Line spacing (m)	Line-km (contractual)	Line-km (delivered)	Flight direction	Line number
BLOCK 1	200	100	100	090°- 270°	L10010-L10300
BLOCK 2	200	77.5	83.5	090°- 270°	L20010-L20280 L60010-L60020
BLOCK 3	200	278.3	278.3	045°- 225°	L30010-L30420
BLOCK 4	200	326.3	326.3	090°- 270°	L40010-L40410
BLOCK 5	200	340.6	340.6	000°- 180°	L50010-L50850

1.5. Survey schedule

Date	Flight #	Block	Nominal Production Km flown	Comments
17-Mar-08	1,2,3	2,1,1	177.5	Production
22-Mar-08	4	3	92.5	Production
23-Mar-08	5,6	3	116.3	Production
27-Mar-08	7,8,9,10	3,4,4,4	374.7	Production
28-Mar-08	11,12,13	4,5,5	205.5	Production
6-Apr-08	14,15,16	5	156.2	Production
7-Apr-08	17	2	6	Production – In-Fills



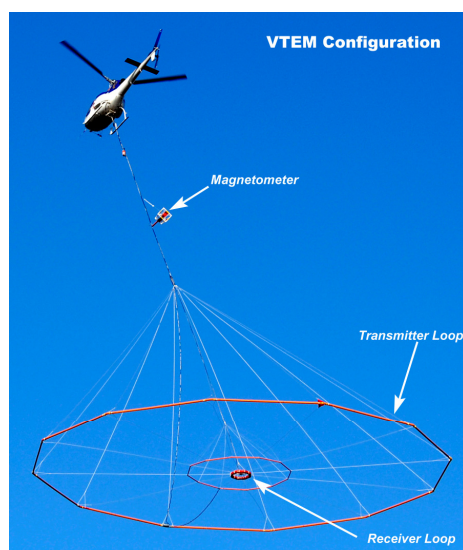
2. SYSTEM SPECIFICATIONS

2.1. Instrumentation

Survey Helicopter	
Model	AS 350 B3
Registration	VH-IPW
Operating Company	United Aero Helicopters
Nominal survey speed	80 km/h
Nominal terrain clearance	80 m
VTEM Transmitter	
Coil diameter	26 m
Number of turns	4
Pulse repetition rate	25 Hz
Peak current	145 Amp
Duty cycle	36.8%
Peak dipole moment	424,528 NIA
Pulse width	7.37 ms
Nominal terrain clearance	34 m
VTEM Receiver	
Coil diameter	1.2 metre
Number of turns	100
Effective area	113.1 m ²
Sampling interval	0.1 s
Nominal terrain clearance	34 m
Magnetometer	
Type	Geometrics
Model	Optically pumped cesium vapour
Sensitivity	0.02 nT
Sampling interval	0.1 s
Cable length	13 m
Nominal terrain clearance	68 m
Radar Altimeter	
Type	Terra TRA 3000/TRI 40
Position	Beneath cockpit
Sampling interval	0.2 s
GPS navigation system	
Type	NovAtel
Model	WAAS enabled OEM4-G2-3151W
Antenna position	Helicopter tail
Sampling interval	0.2 s
Base Station Magnetometer/GPS	
Type	Geometrics
Model	Cesium vapour
Sensitivity	0.001 nT
Sampling interval	1 s



2.2. VTEM Configuration



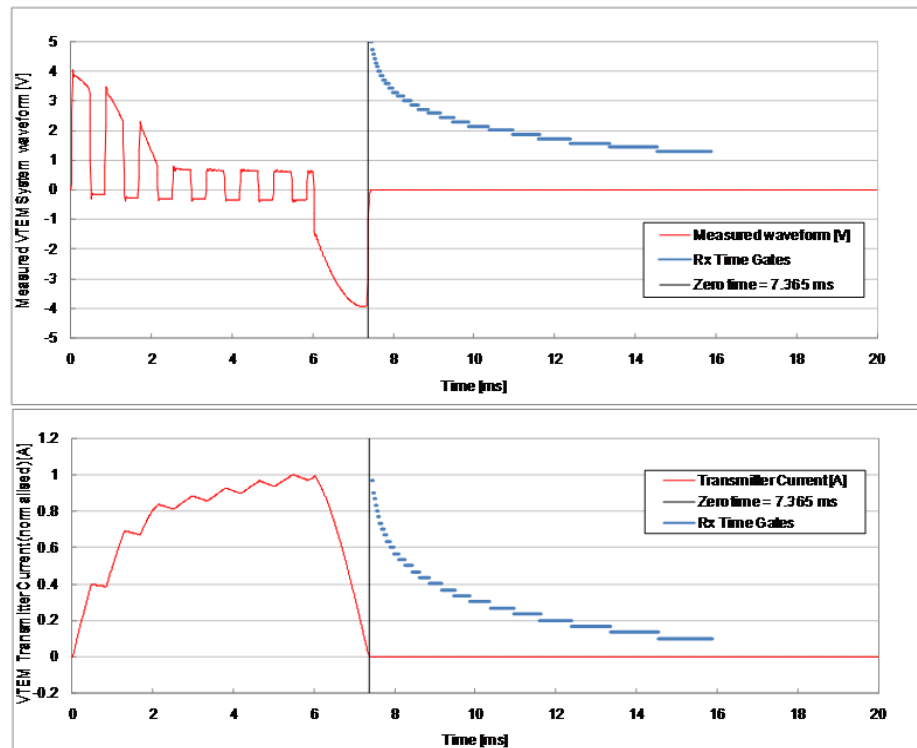
Configuration	
Cable angle with vertical	23 °
Cable length (EM receiver)	42 m
Cable length (Magnetometer)	12 m

2.3. VTEM decay sampling scheme

VTEM B-field System Decay Sampling scheme				
Array Index	Microseconds			
	Middle	Start	End	Width
9	99	91	110	19
10	120	110	131	21
11	141	131	154	24
12	167	154	183	29
13	198	183	216	34
14	234	216	258	42
15	281	258	310	53
16	339	310	373	63
17	406	373	445	73
18	484	445	529	84
19	573	529	628	99
20	682	628	750	123
21	818	750	896	146
22	974	896	1063	167
23	1151	1063	1261	198
24	1370	1261	1506	245
25	1641	1506	1797	292
26	1953	1797	2130	333
27	2307	2130	2526	396
28	2745	2526	3016	490
29	3286	3016	3599	583
30	3911	3599	4266	667
31	4620	4266	5058	792
32	5495	5058	6037	979
33	6578	6037	7203	1167
34	7828	7203	8537	1334
35	9245	8537	10120	1584



2.4. VTEM Transmitter Waveform over one half-period



3. PROCESSING

3.1. Processing parameters

Coordinates	
Projection	MGA Zone 55 S
Datum	GDA 94
Spheroid	GDA 94
Spherics rejection (EM and Magnetic data)	
Non-linear filter	4 point
Non-linear filter sensitivity	0.0001
Low-pass filter wavelength	15 m
Lag correction of other sensors to GPS position	
EM receiver	20 m
Magnetometer	1 m

3.2. Flight Path

The flight path, recorded by the acquisition program as WGS 84 latitude/longitude, was converted into the MGA coordinate system in Oasis Montaj. The flight path was drawn using linear interpolation between x,y positions from the navigation system. Positions are updated every second and expressed as MGA eastings (x) and MGA northings (y).

3.3. Electromagnetic Data

A three stage digital filtering process was used to reject major sferic events and to reduce system noise. Local sferic activity can produce sharp, large amplitude events that cannot be removed by conventional filtering procedures. Smoothing or stacking will reduce their amplitude but leave a broader residual response that can be confused with geological phenomena. To avoid this possibility, a computer algorithm searches out and rejects the major sferic events.

The signal to noise ratio was further improved by the application of a low pass linear digital filter. This filter has zero phase shift which prevents any lag or peak displacement from occurring, and it suppresses only variations with a wavelength less than the specified filter wavelength.

Please note that significant levelling issues were encountered resulting from the presence of power-line interference across blocks 2 to 5 and also moderate terrain variance in block 2.

3.4. Magnetic Data

The processing of the magnetic data involved the correction for diurnal variations by using the digitally recorded ground base station magnetic values. The base station magnetometer data was edited and merged into the Geosoft GDB database on a daily basis. The aeromagnetic data was corrected for diurnal variations by subtracting the observed magnetic base station deviations.



A micro-levelling procedure was applied. This technique is designed to remove persistent low-amplitude components of flight-line noise.

The corrected magnetic data was interpolated between survey lines using a random point gridding method to yield x-y grid values for a standard grid cell size of a quarter of the line spacing. The Minimum Curvature algorithm was used to interpolate values onto a rectangular regular spaced grid.

3.5. Digital Terrain Model

Subtracting the radar altimeter data from the GPS elevation data creates a digital elevation model. Micro levelling technique was employed to level the DEM data.



4. DELIVERABLES

VTEM Survey and logistics report		
Format	PDF	
Copies	2 x Digital (DVD/CD) 2 x Hard copy	
Database		
Format	Digital Geosoft (.GDB)	
Channels	Name	Description
	X	X positional data
	Y	Y positional data
	Lon	Longitude data
	Lat	Latitude data
	Z	GPS antenna elevation (metres above sea level)
	Radar	Helicopter terrain clearance from radar altimeter (metres above ground level)
	Radarb	EM Receiver and Transmitter terrain clearance (metres above ground level)
	DEM	Digital elevation model (metres ASL)
	Gtime	UTC time (seconds of the day)
	Mag1	Raw Total Magnetic field data (nT)
	Basemag	Magnetic diurnal variation data (nT)
	Mag2	Total Magnetic field diurnal variation and lag corrected data (nT)
	Mag3	Leveled Total Magnetic field data (nT)
	Sf[9] to Sf[35]	dB/dt, Time Gates 99 μ s to 9245 μ s (pV/A/m ⁴)
	PLM	Power line monitor
Grids		
Format	Digital Geosoft (.GRD and .GI) ¹	
Grids	Name	Description
	A371_ blk _Mag3	Total Magnetic field (nT)
	A371_ blk _DEM	Digital Elevation Model (m)
Maps		
Format	Digital Geosoft (.MAP and .GM) ²	
Scale	1:25 000 for all blocks	
Maps	Name	Description
	A371_ blk _Mag3	Total Magnetic field
	A371_ blk _DEM	Digital Elevation Model
	A371_ blk _FP	Flight Path
	A371_ blk _EMLog_SF	VTEM dB/dt profiles, Time Gates 0.099 – 9.245 ms in linear - logarithmic scale

¹ A Geosoft .GRD file has a .GI metadata file associated with it, containing grid projection information.

² A Geosoft .MAP file has a .GM metadata file associated with it, containing projection information.



Waveform		
Format	Digital Excel Spreadsheet (VTEM_Waveform.xls)	
Columns	Name	Description
	Time	Sampling rate interval, 10.416 μ s
	Volt	Output voltage of the receiver coil (volt)
	Current	Transmitter current (normalised to 1A peak)

Google Earth Flight Path file	
Format	Google Earth A371 blk Google_KML.kml
	Free version of Google Earth software can be downloaded from, http://earth.google.com/download-earth.html



5. PERSONNEL

Geotech Airborne Limited Personnel	
Operator / Crew chief	Dae Cho
Operator	Jason Callaghan
Technical Support	Andrew Carpenter, David Woodbridge
Data Processing (Preliminary)	Stephen Carter
Data Processing (Final) /Reporting	Alex Castiglione / Simon Bailey
Final data supervision	Stephen Carter Data Processing Manager (stephen.carter@geotechairborne.com.au)
Overall project management	Keith Fisk Managing Partner and Director (keith@geotechairborne.com)



APPENDIX A

GENERALIZED MODELING RESULTS OF THE VTEM SYSTEM (by Roger Barlow)

Introduction

The VTEM system is based on a concentric or central loop design, whereby, the receiver is positioned at the centre of a 26.1 metres diameter transmitter loop that produces a dipole moment up to 625,000 NIA at peak current. The wave form is a bi-polar, modified square wave with a turn-on and turn-off at each end. With a base frequency of 25 Hz, the duration of each pulse is approximately 7.5 milliseconds followed by an off time where no primary field is present.

During turn-on and turn-off, a time varying field is produced (dB/dt) and an electro-motive force (emf) is created as a finite impulse response. A current ring around the transmitter loop moves outward and downward as time progresses. When conductive rocks and mineralization are encountered, a secondary field is created by mutual induction and measured by the receiver at the centre of the transmitter loop.

Measurements are made during the off-time, when only the secondary field (representing the conductive targets encountered in the ground) is present.

Efficient modeling of the results can be carried out on regularly shaped geometries, thus yielding close approximations to the parameters of the measured targets. The following is a description of a series of common models made for the purpose of promoting a general understanding of the measured results.

Variation of Plate Depth

Geometries represented by plates of different strike length, depth extent, dip, plunge and depth below surface can be varied with characteristic parameters like conductance of the target, conductance of the host and conductivity/thickness and thickness of the overburden layer.

Diagrammatic models for a vertical plate are shown in figures A and G at two different depths, all other parameters remaining constant. With this transmitter-receiver geometry, the classic **M** shaped response is generated. Figure A shows a plate where the top is near surface. Here, amplitudes of the dual peaks are higher and symmetrical with the zero centre positioned directly above the plate. Most important is the separation distance of the peaks. This distance is small when the plate is near surface and widens with a linear relationship as the plate (depth to top) increases. Figure G shows a much deeper plate where the separation distance of the peaks is much wider and the amplitudes of the channels have decreased.

Variation of Plate Dip

As the plate dips and departs from the vertical position, the peaks become asymmetrical. Figure B shows a near surface plate dipping 80°. Note that the direction of dip is toward the high shoulder of the response and the top of the plate remains under the centre minimum.

As the dip increases, the aspect ratio (Min/Max) decreases and this aspect ratio can be used as an empirical guide to dip angles from near 90° to about 30°. The method is not sensitive enough where dips are less than about 30°. Figure E shows a plate dipping 45° and, at this angle, the minimum shoulder starts to vanish. In Figure D, a



flat lying plate is shown, relatively near surface. Note that the twin peak anomaly has been replaced by a symmetrical shape with large, bell shaped, channel amplitudes which decay relative to the conductance of the plate.

Figure H shows a special case where two plates are positioned to represent a synclinal structure. Note that the main characteristic to remember is the centre amplitudes are higher (approximately double) compared to the high shoulder of a single plate. This model is very representative of tightly folded formations where the conductors were once flat lying.

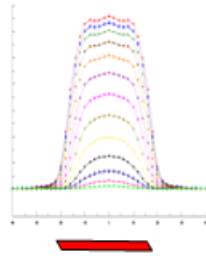
Variation of Prism Depth

Finally, with prism models, another algorithm is required to represent current on the plate. A plate model is considered to be infinitely thin with respect to thickness and incapable of representing the current in the thickness dimension. A prism model is constructed to deal with this problem, thereby, representing the thickness of the body more accurately.

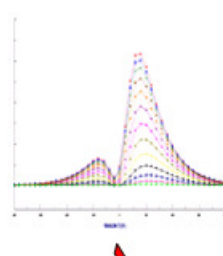
Figures C, F and I show the same prism at increasing depths. Aside from an expected decrease in amplitude, the side lobes of the anomaly show a widening with deeper prism depths of the bell shaped early time channels.



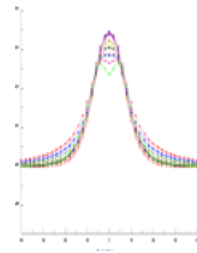
A



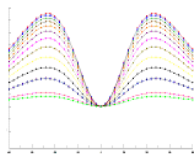
B



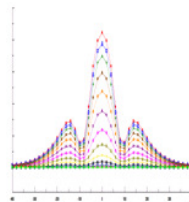
C



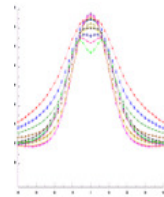
D



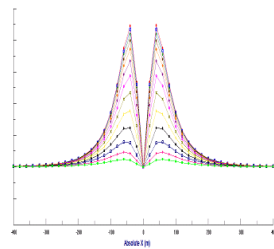
E



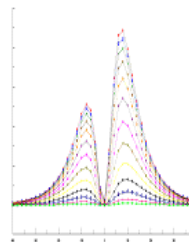
F



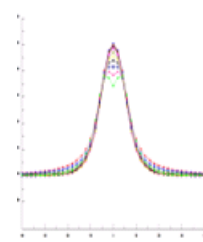
G



H



I



General Modeling Concepts

A set of models has been produced for the Geotech VTEM[®] system with explanation notes (see models A to I above). The reader is encouraged to review these models, so as to get a general understanding of the responses as they apply to survey results. While these models do not begin to cover all possibilities, they give a general perspective on the simple and most commonly encountered anomalies.

When producing these models, a few key points were observed and are worth noting as follows:

- For near vertical and vertical plate models, the top of the conductor is always located directly under the centre low point between the two shoulders in the classic **M** shaped response.
- As the plate is positioned at an increasing depth to the top, the shoulders of the **M** shaped response, have a greater separation distance.
- When faced with choosing between a flat lying plate and a prism model to represent the target (broad response) some ambiguity is present and caution should be exercised.
- With the concentric loop system and Z-component receiver coil, virtually all types of conductors and most geometries are most always well coupled and a response is generated (see model H). Only concentric loop systems can map this type of target.

The modelling program used to generate the responses was prepared by PetRos Eikon Inc. and is one of a very few that can model a wide range of targets in a conductive half space.

General Interpretation Principals

Magnetics

The total magnetic intensity responses reflect major changes in the magnetite and/or other magnetic minerals content in the underlying rocks and unconsolidated overburden. Precambrian rocks have often been subjected to intense heat and pressure during structural and metamorphic events in their history. Original signatures imprinted on these rocks at the time of formation have, in most cases, been modified, resulting in low magnetic susceptibility values.

The amplitude of magnetic anomalies, relative to the regional background, helps to assist in identifying specific magnetic and non-magnetic rock units (and conductors) related to, for example, mafic flows, mafic to ultramafic intrusives, felsic intrusives, felsic volcanics and/or sediments etc. Obviously, several geological sources can produce the same magnetic response. These ambiguities can be reduced considerably if basic geological information on the area is available to the geophysical interpreter.



In addition to simple amplitude variations, the shape of the response expressed in the wave length and the symmetry or asymmetry, is used to estimate the depth, geometric parameters and magnetization of the anomaly. For example, long narrow magnetic linears usually reflect mafic flows or intrusive dyke features. Large areas with complex magnetic patterns may be produced by intrusive bodies with significant magnetization, flat lying magnetic sills or sedimentary iron formation. Local isolated circular magnetic patterns often represent plug-like igneous intrusives such as kimberlites, pegmatites or volcanic vent areas.

Because the total magnetic intensity (TMI) responses may represent two or more closely spaced bodies within a response, the second derivative of the TMI response may be helpful for distinguishing these complexities. The second derivative is most useful in mapping near surface linears and other subtle magnetic structures that are partially masked by nearby higher amplitude magnetic features. The broad zones of higher magnetic amplitude, however, are severely attenuated in the vertical derivative results. These higher amplitude zones reflect rock units having strong magnetic susceptibility signatures. For this reason, both the TMI and the second derivative maps should be evaluated together.

Theoretically, the second derivative, zero contour or colour delineates the contacts or limits of large sources with near vertical dip and shallow depth to the top. The vertical gradient map also aids in determining contact zones between rocks with a susceptibility contrast, however, different, more complicated rules of thumb apply.

Concentric Loop EM Systems

Concentric systems with horizontal transmitter and receiver antennae produce much larger responses for flat lying conductors as contrasted with vertical plate-like conductors. The amount of current developing on the flat upper surface of targets having a substantial area in this dimension, are the direct result of the effective coupling angle, between the primary magnetic field and the flat surface area. One therefore, must not compare the amplitude/conductance of responses generated from flat lying bodies with those derived from near vertical plates; their ratios will be quite different for similar conductances.

Determining dip angle is very accurate for plates with dip angles greater than 30° . For angles less than 30° to 0° , the sensitivity is low and dips can not be distinguished accurately in the presence of normal survey noise levels.

A plate like body that has near vertical position will display a two shoulder, classic **M** shaped response with a distinctive separation distance between peaks for a given depth to top.

It is sometimes difficult to distinguish between responses associated with the edge effects of flat lying conductors and poorly conductive bedrock conductors. Poorly conductive bedrock conductors having low dip angles will also exhibit responses that may be interpreted as surficial overburden conductors. In some situations, the conductive response has line to line continuity and some magnetic correlation providing possible evidence that the response is related to an actual bedrock source.

The EM interpretation process used, places considerable emphasis on determining an understanding of the general conductive patterns in the area of interest. Each area has different characteristics and these can effectively guide the detailed process used.



The first stage is to determine which time gates are most descriptive of the overall conductance patterns. Maps of the time gates that represent the range of responses can be very informative.

Next, stacking the relevant channels as profiles on the flight path together with the second vertical derivative of the TMI is very helpful in revealing correlations between the EM and Magnetics.

Next, key lines can be profiled as single lines to emphasize specific characteristics of a conductor or the relationship of one conductor to another on the same line. Resistivity Depth sections can be constructed to show the relationship of conductive overburden or conductive bedrock with the conductive anomaly.



APPENDIX B
GEOPHYSICAL MAP IMAGES
(not to scale)



